ISSN (Print) 1226-1750
ISSN (Online) 2233-6656
Journal of Magnetics 23(3), 392-398 (2018) https://doi.org/10.4283/JMAG.2018.23.3.392

Design of an Electromagnetic Energy Harvesting System Applied to Shock Absorber in Sport Utility Vehicle: Part II. Improvement of The Power & Power Density

Minh-Trung Duong[1,2] and Yon-Do Chun[1,2]*

[1]*University of Science and Technology, Yuseong-gu, Daejeon 34113, Korea*
[2]*Korea Electrotechnology Research Institute, Seongsan-gu, Changwon 51543, Korea*

(Received 4 April 2018, Received in final form 12 September 2018, Accepted 14 September 2018)

To harvest the kinetic energy from the vehicle suspension system, a tubular generator, which is composed of a single permanent magnet layer coreless model, was proposed in the previous study. Despite the excessive volume of the generator, both output power and power density are significantly lower than other conventional machines. This paper examines different designs of the tubular generator with the goal to enhance the performance, including a double permanent magnet layers coreless model and a cored model. By using a commercial finite element method (FEM) software, two proposed generators are theoretically analyzed and compared with the conventional generator. Analyzed results reveal that under the same operating conditions, the cored model can regenerate the largest amount of the power density. These results indicate that cored model can be considered as a promising candidate for the application to the electromagnetic shock absorber in sport utility vehicle (SUV).

Keywords : Electromagnetic energy harvesting, tubular machine, Halbach array, shock absorber

1. Introduction

The tubular generator has been applied to the energy harvesting system in the electric vehicle due to its simple structure, neglection of the mechanical loss and high power conversion efficiency [1-13]. Different from the goal to replace the traditional shock absorber by the novel electromagnetic shock absorber in the other researches [1, 2, 13], the proposed device in the [3] is a semi-active shock absorber, which is a combination of the electrical components and mechanical components. In the detail design, a permanent magnet (PM) layer is mounted to the inner frame of the shock absorber, while windings are attached to the outer frame. This configuration leads to the excessive volume of the generator, in which outer diameter is 160 mm and total length is 264 mm. However, the output power and power density values are relatively lower than those in the conventional design [1, 2] because of the large electrical airgap, which is 12.4 mm, and an excessive volume.

To enhance the performance, it is necessary to increase the magnetic flux density in the coil windings. Theoretically, if the flux density is increased by two times, the output power is correspondingly increased by four times [2]. In this paper, a tubular generator using double PM layers, coreless type is designed and compared with the conventional single PM layer machine in terms of flux density, output power, and power density. In addition, another machine using the magnetic material for the coil slot, this is named cored type, is also considered. The analytical results reveal that under the same operating conditions, the cored model can regenerate dramatically greater power density than the other two coreless machines. However, one of the most critical shortcomings of the cored type is its excessive electromagnetic force, which effects to the safety and driving comfort.

In the further study, the investigation on the reduction of machine's volume and electromagnetic force, enhancement of the power and power density of the cored type will be taken into account.

*Corresponding author: Tel: +82-55-280-1427
Fax: +82-55-280-1490, e-mail: ydchun@keri.re.kr

2. Design Specification

2.1. Double PM layers coreless machine

Figure 1 shows the half cross-section of the single PM layer coreless model again by using the same theory and basic design in [1-3], and the cross-section of the double layers coreless model is shown in Fig. 2 and Fig. 3. Instead of being excited by only inner PM layer, armature coil in the double PMs layers machine is inserted between an inner PM layer and an outer PM layer, in which both layers are also composed of the Halbach array. Because of the non-magnetic material for the coil slots, electrical airgap is 14.5 mm. To simplify the comparison between different machines, various design parameters are still

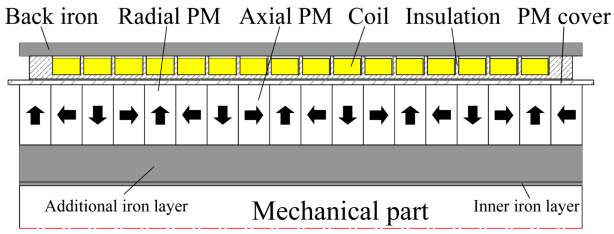

Fig. 1. (Color online) Half cross-section of the single PM layer coreless model.

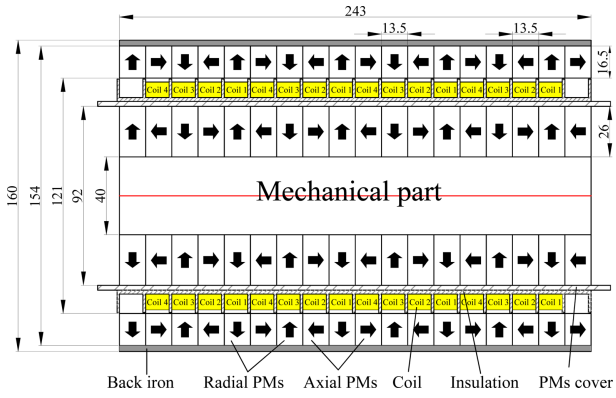

Fig. 2. (Color online) Cross-section of the full double PM layers coreless model.

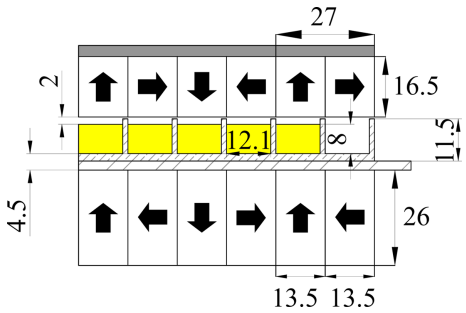

Fig. 3. (Color online) Dimensions of the double PM layers coreless machine.

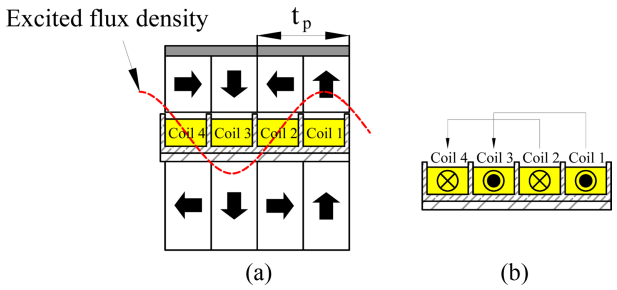

Fig. 4. (Color online) (a) Relative position between the coil winding and excited flux density; (b) Coil windings with connection and current direction.

remained from the previous design of the single PM layer machine, including outer diameter, total length, pole pitch and the width of the PMs. It should be noted that the ratio between slot pitch and pole pitch is 1 : 2. In addition, the proposed machine is theoretically composed of 16 slots and 8 poles, however there is one additional pole to ensure that during the vibration, armature windings are always inside the electromagnetic field.

Due to the relative position of the excited flux density as shown in Fig. 4, there are totally 16 coils, in which coil 1 and coil 3 (0° coils & 180° coils) are in the series connection, this is named phase 1, coil 2 and coil 4 (90° coils and 270° coils) are in the series connection, this is name phase 2. In order to achieve the maximum output power, current on phase 1 and phase 2 are in the opposite direction.

Although the design with double PM layers using Halbach array is possible to increase the output power and power density [2], one of the major drawbacks to exploiting this system is its excessive volume. The outer diameter of the single PM layer [3] and the proposed double PM layers in this paper were designed to be 160 mm. While the prototypes of the conventional electromagnetic shock absorber in the other studies have been successfully investigated and fabricated based on the dimensions of the traditional shock absorbers, in which outer diameter is only around 76 mm [1, 2, 13].

Design specifications of the conventional single PM layer, double PM layers coreless and cored machine are summarized in Table 1.

2.2. Cored machine

This section presents a novel configuration of the cored type tubular machine with the targets to reduce the volume and increase the output power and power density. The most remarkable difference between the conventional coreless machine and novel cored machine is the replacement of the Bobbin material, a non-magnetic material

Table 1. Design specifications of the three comparative machines.

Item	Values		
	Single PM layer	Double PM layers	Cored model
Length, L (mm)	243	243	243
Outer diameter, D (mm)	160	160	110
Inner PMs diameter, D_{im} (mm)	72	40	40
Inner PM thickness, t_{im} (mm)	26.0	26.0	15.0
Outer PM thickness, t_{om} (mm)	–	16.5	–
Radial PM width, w_{rm} (mm)	13.5	13.5	13.5
Axial PM width, w_{am} (mm)	13.5	13.5	13.5
Pole pitch, τ_p (mm)	27.0	27.0	27.0
Coil window thickness, t_c (mm)	8.0	8.0	12.3
Coil window width, w_c (mm)	12.1	12.1	5.5
Inner electrical airgap, g_i (mm)	12.4	14.5	0.7
Back iron thickness, t_b (mm)	5.6	3.0	5.0
Wire diameter, w_r (mm)	0.6	0.6	0.6
Number of winding/slot (turns)	180	216	152
Resistance (one phase), R (Ω)	19.2 (at 20 °C)	18.0 (at 20 °C)	9.96 (at 20 °C)
Back iron material	S20C		
PMs material	NdFeB – N40SH : B_r = 1.26T; μ_r = 1.05		

using for coil slots, by S20C, a commercial magnetic steel. This particular structure was chosen on account the fact that flux linkage can be significantly increased thanks to the high relative permeability of the magnetic material.

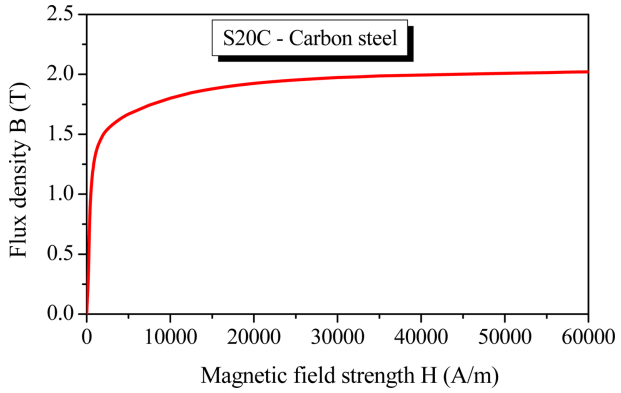

Fig. 5. (Color online) B-H curve of the carbon steel S20C.

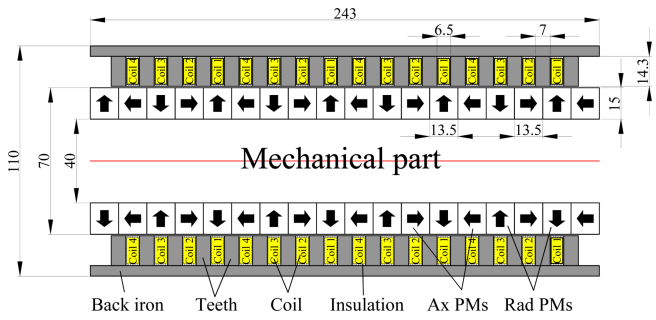

Fig. 6. (Color online) Cross-section of the cored type tubular machine.

Therefore, machine's performance can be improved, while it is possible to reduce the volume.

The B-H curve of the S20C and overview of the novel cored type tubular machine are shown in Fig. 5 and Fig. 6, respectively.

As the depiction in Fig. 6, the total length of the cored type tubular machine was fixed to be 243 mm, but its outer diameter was reduced to be 110 mm. Similar to the previous design in [3], the cored model consists of a single PM layer mounted on the body of the mechanical part, an armature winding, which is wound and supported by iron teeth and outer back iron. In this design, to economize the cored model, the thickness of the PMs was selected to be only 15 mm, by nearly a half than that of the double PM layers machine, while the inner diameter was fixed to be 40 mm. It is estimated that the total volume of the PMs in the cored model is reduced by 3.09 times and 4.83 times than it is in the single PM layer and double PM layers machine, respectively. Ideally, the pole pitch, and PMs width are remained to be the same as the previous designs.

Another problem was successfully solved in this section is reduction of the large electrical airgap because of the use of the non-magnetic material in the previous designs. Instead of using a stainless steel cover to wrap around the surface of the PMs, two layers of the carbon fiber were considered. One of the major advantages of the carbon fiber is relatively sleazy thickness, which is only 0.1 mm for one layer, but it still ensures the mechanical strength. Including 0.5 mm of the mechanical airgap, the total

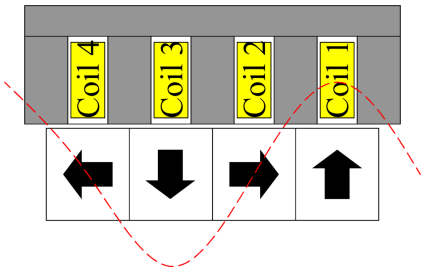

Fig. 7. (Color online) Relative position between coil phases and flux distribution.

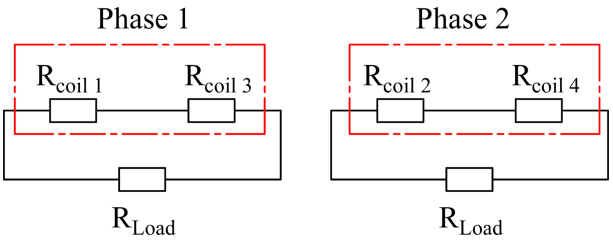

Fig. 8. (Color online) External circuit connection.

electrical airgap in the proposed machine is reduced to be 0.7 mm.

For the winding connection and external circuit, the novel cored model is also designed as a 2-phase machine based on the same slot-pole combination, the relative position between armature windings and excited flux density as the depictions in Fig. 7 and Fig. 8. The major differences in this part are dimensions of the coil slots and the number of turns.

3. FEA Characterization

3.1. Operating conditions

With the target to harvest the dissipated kinetic energy from the suspension system [3] in an SUV car, it is assumed that a medium size car is moving on the road class C at a speed of 60 mph (96 km/h). Under these conditions, proposed tubular machine, which is directly assembled with the shock absorber in the vehicle, is operated with 0.25 m/s of the vibrating speed, 10 Hz of the vibrating frequency and 11.25 mm of the peak to peak stroke length. The software package used to analyze data was Flux 2D provided by Altair company. To control the vibrating motion with above parameters, an equation of the position of the moving part was input as follows:

$$x = \frac{11.25}{2} \times 10^{-3} \times \mathrm{Sin}(2\pi \times 10 \times t)(\mathrm{mm}) \quad (1)$$

Different from the linear machine, which is operated by the linear motion, the tubular machine in application to

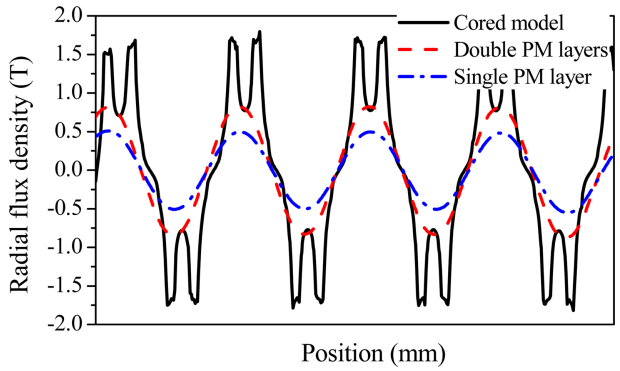

Fig. 9. (Color online) Radial flux density.

the energy harvesting field in the vehicle suspension system has to be controlled by vibrating motion. This is a reason to explain why an extreme caution must be taken when setting up the exact initial position for both analysis and experiment, otherwise, the output power can be eliminated and voltage waveform can be distorted [3]. Although the application of the tubular machine in the energy harvesting field is generating considerable interest, there are only a few researchers have addressed the problems with the vibrating motion.

3.2. Magnetic flux density

The first set of analyses highlighted the radial magnetic flux density between three machines as shown in Fig. 9, in which it was measured in the middle of the coil in case of the coreless models and in the middle of the electrical airgap in the cored model. It can be clearly seen that maximum flux density of the cored model is extremely higher than those of the double PM layers and single PM layer in spite of the smaller PMs volume, which are 1.82 T, 0.88 T, and 0.55 T, respectively. These values correlate satisfactorily well with X. Tang [2] that flux density can be increased by using double PM layers configuration.

3.3. No-load induced voltage

The no-load induced voltage or back EMF waveforms on each phase are compared in Fig. 10. While the frequency of the back EMF on phase 1 is 10 Hz according to the initial design, it is 20 Hz in phase 2. Identically, this characteristic is theoretically consistent with previous results [1-3], which presented the unbalanced back EMF between phase 1 and phase 2 because of the relative position between coil winding and excited flux density.

With the highest PM volume, peak values of the no-load induced voltage from the double PM layers on phase 1 and phases 2 are maximum, which are 167.44 V and 59.55 V, respectively. Interestingly, despite the fact that the PM volume in the cored model is less than it is in the

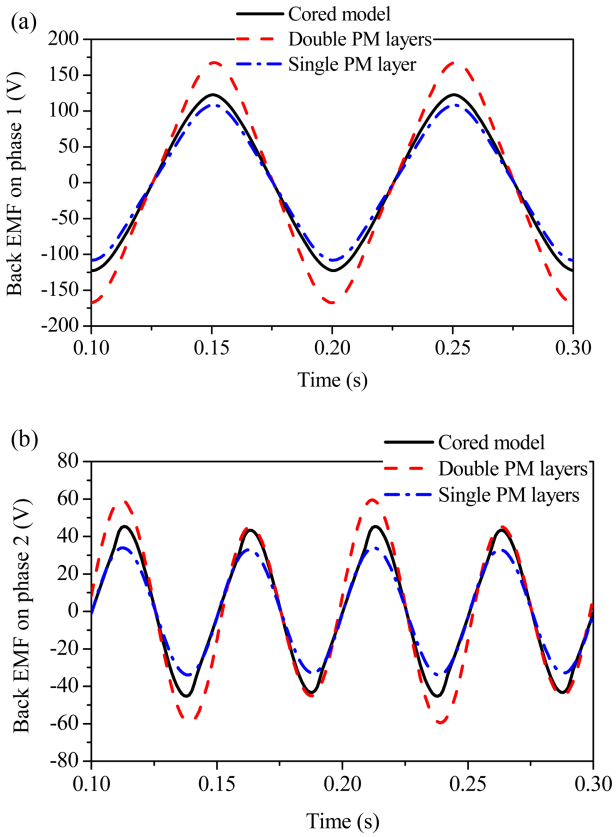

Fig. 10. (Color online) No-load voltage on: (a) phase 1; (b) phase 2.

single PM layer by 3.09 times, maximum back EMF on phase 1 and phase 2 from the cored model are higher by approximately 13.3 % and 33.5 %, respectively.

3.4. Power and power density

To maximize the output power, the load resistance is installed to be the same as the coil winding resistance [3]. As anticipated, under the full load condition, maximum harvestable power is from the double PM layers, in which maximum output power is about 195.00 W and average

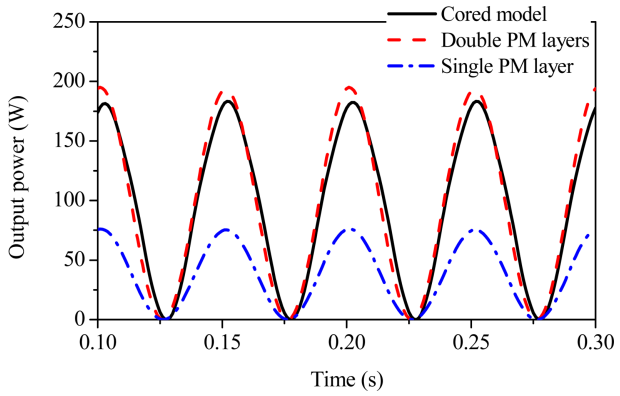

Fig. 11. (Color online) Comparison of the output power between three machines.

output power is around 96.65 W. The power waveforms and values are compared in the Fig. 11.

The most striking results to emerge from the data is that power density has been significantly increased in case of the cored model. Moreover, volume of the PM in the cored model is significantly reduced. For example, as illustration in Fig. 6, the length, inner and outer diameter of the PM are 243, 40 and 70 mm, respectively. The total volume is calculated by the following equation:

$$V_{PM} = \frac{\pi \times (70^2 - 40^2)}{4} \times 0.243 = 629.8(\text{cm}^3)$$

Similarly, volume of the PM in the double and single layer model are 3,042 and 1,945.2 cm^3. Volume of the other electrical components are calculated by the same approach. It should be noted that active volume is assumed to be the summation of the PMs, iron core, copper, and electrical airgap. While the total volume of the double PM layers and single PM layer are estimated by around 4780.45 cm^3 and 3334.30 cm^3, the total active volume of the cored model is only 1708.56 cm^3. This leads to the huge gap between three models in terms of the power density. The maximum power density of the double PM

Table 2. Performance of the three comparative machines.

Item	Values		
	Single PM layer	Double PM layers	Cored model
Maximum flux density (T)	0.55	0.88	1.82
RMS flux density (T)	0.36	0.59	1.05
Maximum output power (W)	76.14	195.00	183.24
Average output power (W)	37.79	96.65	94.56
Maximum power density (W/cm^3)	0.023	0.041	0.107
Average power density (W/cm^3)	0.011	0.020	0.055
Maximum cogging force (N)	46.55	1.00	2135.49
Maximum electromagnetic force (N)	474.42	1103.34	3048.88

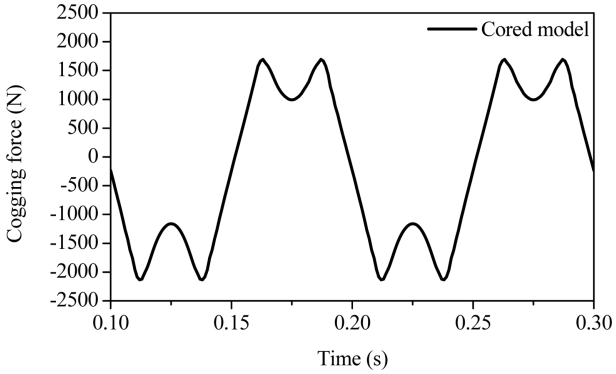

Fig. 12. Cogging force of the cored model.

layers and single PM layer are about 0.041 W/cm^3 and 0.023 W/cm^3, respectively, while in case of the cored model, it is about 0.107 W/cm^3. These analyzed results suggest that a tubular machine using the magnetic iron core for the coil teeth is a promising candidate in terms of the power density. Performance of the three comparative machines is summarized in Table 2.

3.5. Electromagnetic force

In case of the single PM layer structure, the interaction between PMs and back iron results a maximum cogging force of 46.55 N. Cogging force can be eliminated in case of the double PM layers because the armature winding is totally supported by the Bobbin, a non-magnetic material. Despite the excellent power density, the major shortcoming of the cored model occurs from the electromagnetic force, which leads to the negative effects on the safety and drives comfort. As detailed in Fig. 12, maximum cogging force can reach to the peak of 2135.49 N.

Figure 13 compares the electromagnetic force under the full-load condition between three machines according to the position of the moving part. Analyzed results indicate the maximum force of the cored model, double PM layers

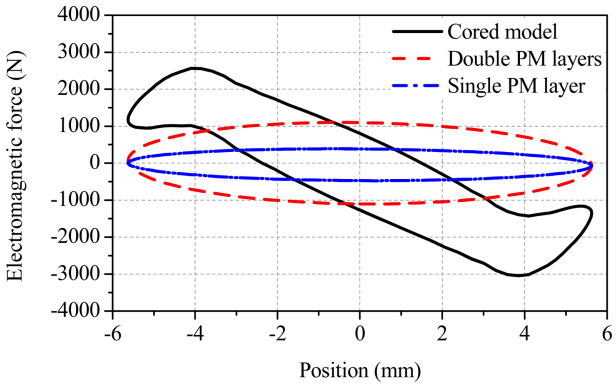

Fig. 13. (Color online) Electromagnetic force between three machines for different position of the moving part.

and single PM layer are approximately 3048.88 N, 1103.34 N and 474.42 N, respectively. It probable that although the electromagnetic force can be reduced by various classical approaches, a trade-off point, which is satisfied with the balance between output power and force, should be taken into account.

4. Conclusion

Considerable insight has been gained with regard to the improvement of the performance of the tubular machine, especially power density. There are two different machines proposed in this paper, including a double PM layers coreless model and a cored model. This work has revealed that under the same operating condition, although the PM volume is significantly reduced, the cored model can possibly generate higher power density value than the double PM layers and the single PM layer machine by 2.6 times and 4.7 times, respectively. Results so far have been very encouraging and suggest that a tubular machine using the magnetic material for the coil teeth is a promising candidate for the energy harvesting application to the vehicle suspension system. The most important limitation lies in the excessive electromagnetic force, which has a linear proportion of the output power. Research into solving this problem is already underway using multi-objective optimization or applying various classical approaches, such as skewing effect, pole-shoes geometry for the iron teeth and so on. Further work needs to be done with the corresponding experimental data to validate the accuracy of the calculation, therefore, several prototypes will be fabricated and tested.

Acknowledgement

This work was made possible by a grant from Civil-Military Technology Cooperation Program (No.: 16-CM-EN-17) funded by the Defense Acquisition Program Administration and the Ministry of Trade, Industry & Energy in Korea.

References

[1] L. Zuo, B. Scully, J. Shestani, and Y. Zhou, Smart Mater. Struct. **19**, 045003-1-045003-10 (2010).
[2] X. Tang, T. Lin, and L. Zuo, IEEE/ASME Trans. Mecha. **19** (2014).
[3] M. T. Duong, Y. D. Chun, P. W. Han, B. G. Park, D. J. Bang, and J. K. Lee, J. Magn. **22** (2017).
[4] P. Li, L. Zuo, J. Lu, and L. Xu, 2014 IEEE Int. Conf. Sys., Man, and Cybernetics (2014).
[5] Z. Li, L. Zuo, G. Luhrs, L. Lin, and Y. X. Qin, IEEE.

Trans. Veh. Technol. **62** (2013).
[6] E. Asadi, R. Ribeiro, M. B. Khamesee, and A. Khajepour, Smart Mater. Stuct. **24**, 075003 (2015).
[7] X. Tang and L. Zuo, J. Intell. Mater. Syst. Struct. **23**, 2117 (2012).
[8] L. Zuo and P. Zhang, in Proc. DSCC, 295 (2012).
[9] P. S. Zhang, Master of Science Thesis (2010).
[10] Y. Liu, Doctor of Philosophy Thesis (2016).
[11] L. Zuo, X. Tang, and P. Zhang, U. S. Patent 31/368846, filed 07.2011.
[12] R. B. Goldner and P. Zerigian, United States Patent, Patent No: 6,952,060 B2, Date of Paten: Oct. 4 (2005).
[13] B. L. J. Gysen, J. L. G. Jansen, J. J. H. Paulides, and E. A. Lomonova, IEEE Trans. Ind. Appl. **45** (2009).